Michigan State University

National Superconducting Cyclotron Laboratory

HIGH ENERGY GAMMA RAY PRODUCTION IN PROTON INDUCED REACTIONS AT 104, 145, AND 195 MeV

J. CLAYTON, W. BENENSON, M. CRONQVIST, R. FOX,
D. KROFCHECK, R. PFAFF, T. REPOSEUR,
J.D. STEVENSON, J.S. WINFIELD, B. YOUNG,
M.F. MOHAR, C. BLOCH, and D.E. FIELDS

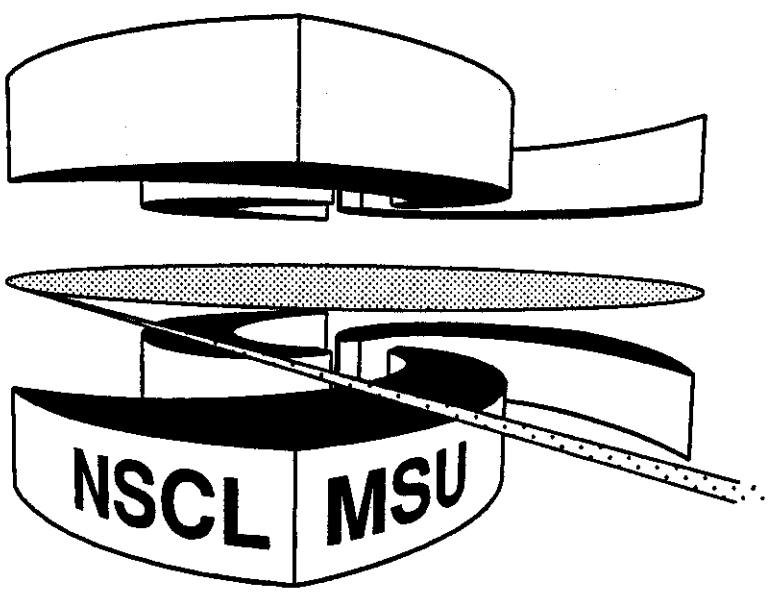

MSUCL-800

NOVEMBER 1991

MSUCL-800
November, 1991

High Energy Gamma Ray Production in Proton Induced Reactions at 104, 145 and 195 MeV

J. Clayton[§], W. Benenson, M. Cronqvist*, R. Fox,
D. Krofcheck[†], R. Pfaff, T. Reposeur[‡], J.D. Stevenson[§],
J.S. Winfield and B. Young

National Superconducting *Cyclotron Laboratory and*
Department of Physics *and Astronomy,* Michigan *State University*
East Lansing, Michigan 48824

M.F. Mohar

National *Superconducting Cyclotron Laboratory and*
Department of Chemistry, Michigan State University
East Lansing, Michigan 48824

C. Bloch and D. E. Fields

Indiana University Cyclotron Facility
Bloomington, Indiana 47405

Energy spectra and angular distributions have been measured for high energy gamma rays ($E_\gamma \geq 20$ MeV) from proton-nucleus reactions at 104, 145 and 195 MeV on targets of C, Zn and Pb. Gamma rays were observed with energies up to 170 MeV. The spectra showed differences from the typical exponential shape that is observed in gamma ray production from heavy-ion reactions. The angular distribution of the gamma rays is forward peaked in the laboratory, which is consistent with emission from a moving source. A comparison is made with previous measurements at 72, 140, 168, and 200 MeV. The experimental evidence indicates that first chance incoherent proton-neutron bremsstrahlung is the main production mechanism.

I. INTRODUCTION

Understanding the proton–nucleus bremsstrahlung mechanism is important for a number of reasons; first and foremost is that studies of this reaction can lead to a greater comprehension of the more fundamental reaction pnγ. Secondly, proton–nucleus reactions can also improve our understanding of the more complicated reaction dynamics associated with bremsstrahlung reactions in nucleus–nucleus collisions. The recent reports on high energy gamma ray production in heavy–ion reactions by several experimental groups [1–6] has caused research groups to scrutinize earlier proton induced data much more carefully. Theoretical calculations [7–9] of bremsstrahlung in heavy ion reactions have used the available proton-nucleus data as a gauge for their calculations before attacking the more involved calculations required to explain the production of photons in heavy-ion induced reactions.

The characteristics of the energy spectra and angular distributions of the photons emitted during these heavy-ion reactions lead experimenters to conclude that the photons were coming from incoherent proton–neutron bremsstrahlung [4, 5]. The elementary proton–neutron bremsstrahlung (pnγ) is much more efficient than proton–proton (ppγ) bremsstrahlung in the production rate of high energy gamma rays, and this fact makes the pnγ cross section an important quantity in the theoretical models of high energy gamma ray production. There are very few data sets in the literature on neutron-proton bremsstrahlung [10–12]. Genuine npγ measurements require neutron beams of high intensities and well defined energies. This is complicated by the fact that the data on npγ are poor; only double differential cross sections $d^2\,\sigma/d\,\Omega_p\,d\,\Omega_n$ are available at a small number of angles for n + H reactions at 208 MeV [10] and 130 MeV [11]. The statistics of these measurements are not sufficient for the detailed knowledge of the angle-integrated cross sections necessary for heavy-ion calculations.

Information on the pnγ process in heavy-ion reactions can also be deduced from

proton-nucleus reactions. In this case the solution to the phase space problem is easier since consideration has to be given only to the target nucleons which allows the testing of different theoretical models of the reaction dynamics. Experimental data in this area have been sorely lacking until recently. The first systematic study of target and angle dependence of high energy gamma ray production in proton–nucleus reactions was completed by Edgington and Rose [13]. In this work 140 MeV protons were incident on various targets ranging from deuterium to lead. The p + d result is fundamental because it should be a reasonable approximation to the free pnγ value. At the same time the pdγ result can also yield information on phase space considerations necessary for proton-nucleus reactions. These ideas can then be extended to explain bremsstrahlung photons produced in heavy-ion reactions. The results from the Edgington and Rose measurement were thought to be correct until measurements by Kwato Njock *et al.* at 72 MeV [14] and Pinston *et al.* at 168 and 200 MeV [15]. In these works, the authors found a discrepancy between their measurements and those of Edgington and Rose. It should be noted that the detector system used by both Kwato Njock *et al.* and Pinston *et al.* was a BaF_2 + NaI(Tl) telescope [16]. The results of Edgington and Rose for the deuterium target were also in disagreement with an experiment performed by Koehler, Rothe and Thorndike at 197 MeV [17]. The important features from the Edgington and Rose measurement which still hold in the later measurements were that the shapes of the spectra were similar for all the targets. The total cross section for the various targets can be scaled with a simple $N/A^{1/3}$ dependence where N and A are the number of neutrons and atomic number of the target. This is similar to the $(A_p \cdot A_t)^{2/3}$ dependence observed for gamma ray production in heavy-ion reactions. The angular distributions of the bremsstrahlung gamma rays in the laboratory were found to be fall off less sharply with energy for forward angle emission. All of these characteristics lead the authors of Refs. [13–15] to conclude

that the origin of the gamma rays were incoherent proton–neutron bremsstrhalung.

The objective of the experiment discussed in the present paper was to study photon production for proton induced reactions at several incident beam energies and to measure the total cross section for these bremsstrahlung photons, thereby answering the questions about the discrepancy between the earlier data of Edgington and Rose and the more recent measurements by Kwato Njock *et al.* and Pinston *et al.* . Data on p + d bremsstrahlung taken at the same time will be discussed in a separate paper.

II. EXPERIMENT

The energy spectra and angular distribution of gamma rays were measured in the energy range between 10 and 170 MeV. The gamma ray detectors were the same two large BaF_2 detectors [18] which were previously used to measure high energy gamma rays produced in heavy-ion reactions [19]. The detectors consisted of two right cylinders of BaF_2 , 12.7 cm (2.9 ρ_m- Molière radius) in diameter and 11.45 cm in length. The optical joint between the crystals was made with 100,000 centipoise silicon oil [20]. The total length of the detectors was 22.9 cm which is 11.2 radiation lengths (L_{rad}=2.05 cm). The acceptance diameter for each detector was determined by an 11.5 cm deep 95% tungsten collimator which was tapered to cover a constant solid angle at 75 cm from the target. The solid angle coverage for each detector was 11 msr. The detectors were surrounded by a 2.54 cm plastic anticoincidence shield which was used to reject charged particles coming from the target as well as the significant background from cosmic ray muons. Prompt particles from the target were attenuated by the use of high density polyethylene bars placed in between the target and the detector. At forward angles, $\theta_{lab} < 90$ °, the detectors were operated with a 40 cm polyethylene bar while a 20 cm bar was employed for the other angles.

Fast neutrons and charged particles which pass through the absorber bar were rejected on the basis of their time-of-flight relative to the cyclotron RF. The time resolution for the BaF_2 detector is approximately 850 ps full width at half maximum (FWHM) for gamma rays above 10 MeV but is limited by the width of the cyclotron RF pulse. The final cut on rejecting background events was made with the pulse shape information available with the BaF_2 crystal scintillation light output. The detector response to high energy gamma rays was calibrated at the tagged photon facility at the Saskatchewan Accelerator Laboratory. The details of the tagged photon experiment and the Monte-Carlo studies using the electromagnetic shower code EGS4 [21] can be found in Ref. [22].

Proton beams of 104, 145 and 195 MeV from the Cyclotron at the Indiana University Cyclotron Facility (IUCF) bombarded targets of self-supporting foils of C, Zn and Pb. The thicknesses for the targets ranged from 25 mg/cm^2 for the Zn and Pb targets to 31 mg/cm^2 for the C target. For all the beam energies, measurements were made at laboratory angles of 60°, 90° and 120° with additional angles at 45° and 135° for some of the targets and incident proton energies. Since the data at all the beam energies used the same targets, the energy dependence for the various targets could be examined. Both detectors were used for some of the angles which permitted extensive cross checking of the data. The beam intensity at IUCF was on the order of 6×10^{10} protons/sec, and was monitored by a Faraday cup. Online calibration of the energy scale was done with the 15.1 MeV γ -ray transition from the ^{12}C target. Long runs with cosmic ray muon energy deposition in the BaF_2 crystals were also performed prior to the beginning of the experiment, during beam energy changes, and at the end of the measurement. The energy deposition of cosmic ray muon along the diameter of the BaF_2 crystal is 81 MeV which is approximately one half of the full scale energy used in this experiment.

III. RESULTS AND DISCUSSION

A. Comparison with Moving Source Model

The gamma ray energy spectra in the laboratory frame for three of the measured angles at 104 MeV and 145 MeV are shown in Fig. 1. The spectra display a tendency to fall off less sharply with energy for forward angle emission. The angular distributions in the laboratory frame for photons above 40 MeV are typically forward peaked. The ratios of the energy integrated cross section at $\sigma(60°)/\sigma(120°)$ at 145 MeV for C, Zn and Pb are 2.3, 1.6 and 1.7 respectively. The source velocity for the 104 and 145 MeV data was extracted from a contour plot of the invariant cross section versus the rapidity $y = 1/2 \ln\left((E + P_{\|})/(E - P_{\|})\right)$ and the transverse momentum $P_{\perp} = E_{\gamma} \cdot \sin(\theta)$, where θ is the photon observation angle. A fit was then made to the contours of constant invariant cross section with a second order polynomial. The values for the centroid of the rapidity is close to the nucleon-nucleon center-of-mass rapidity for both incident proton energies. The results for the centroids for all the targets are displayed in Table I. The centroid of the rapidity distribution tends to decrease as the energy of the photon increases. This trend can be explained within the framework of incoherent proton-neutron bremsstrahlung as an interaction of a neutron in the target which has its Fermi momentum vector pointing in a direction opposite to the incident proton momentum vector. In such a collision the source velocity becomes less than the nucleon–nucleon center-of-mass velocity.

A systematic analysis was performed to extract various quantities of interest such as the strength of the dipole component or the existence of any quadrupole component in the angular distribution. Fits to the energy spectra were made with a moving source model which will also yield a value for the emission source velocity. The original expression for the bremsstrahlung cross section formulated by Nakayama and Bertsch [9] was an attempt to combine into one simple expression, the asymptotic behavior

of the energy spectra at both the low and high energy portion of the spectrum. Nakayama and Bertsch wanted to have a qualitative expression for comparison to the more sophisticated calculation they were doing. For low energy photons, the energy dependence is the usual classical bremsstrahlung result namely, $1/E_\gamma$, while near the maximum photon energy, the bremsstrahlung cross section is proportional the final state phase space available. In the Fermi Gas Model, the density of states of a given particle–hole character varies as the power of the excitation energy. In the case of proton–neutron collisions the final state has a 2-particle 1-hole character. This results in the bremsstrahlung cross section near the endpoint having a dependence on the gamma ray energy, as $(E_{max} - E)^2$ [23]. Nakayama and Bertsch combined the limiting behavior into one function:

$$\frac{d^2\sigma}{dEd\Omega} \propto G(\theta) \cdot \left(\frac{(E_{max} - E)^2}{E_{max} E} \right) \tag{1}$$

where $G(\theta) = 0.6 \cdot \sin^2(\theta) + 0.4$, which is the predicted isotropic plus dipole angular distribution. Nakayama and Bertsch chose the normalization such that the angular distribution would be unity at 90°. The expression used in the present work for the double differential cross section in the least squares fit was a modified expression of Nakayama and Bertsch's and is given by:

$$\frac{d^2\sigma}{dEd\Omega} = N \cdot \left(\frac{(E_{max} - E)^\lambda}{E_{max} E} [1.0 + a_2 P_2(cos(\theta)) + a_4 P_4(cos(\theta))] \right) \tag{2}$$

The modifications to the original phase space model of Nakayama and Bertsch were the addition of the quadrupole component and allowing the exponent, λ, to vary. Also, with this model a source velocity could be extracted. Proper treatment of the maximum gamma ray energy was completed by including the Fermi momentum of the target neutrons and Pauli blocking effects. This leads to an increase of the maximum gamma ray energy in the emitting frame which permits the calculation to fit all the angles simultaneously. If the Fermi momentum of the target neutrons was not taken

into account it would not be possible to fit the backward angle data due to the effect of the Lorentz transformation.

The least-squares fits to the energy spectra were performed with the minimization package MINUIT [24]. It should be noted that the fitted spectra are folded with the response function for the detector which was calculated with the code EGS4 and compared with the tagged photon data. The quality of the fits is displayed in Fig. 2 for C and Pb targets at an incident proton energy of 145 MeV. The agreement between the theoretical curve and the data improves as the target mass is increased. The values for the reduced χ^2 varies from 7.2 for the C to 1.2 for the Pb target and is attributed to the fact that the phase space model uses infinite nuclear matter approximations; in fact the value of λ approaches the predicted infinite nuclear matter value of two as the target mass is increased. The values of λ varies from 1.0 ± 0.2 for the C targets to 1.8 ± 0.2 for the Pb target. The extracted source velocity is found to be the nucleon center-of-mass velocity $\beta_{nn} = 0.23$ for all the targets at the incident proton energy of 104 and $\beta_{nn} = 0.27$ for all the targets at 145 MeV. The data at 195 MeV was not fit at all. This was because there was a large background of gamma rays coming from π^0 decay. The contribution to the total photon cross section for gamma ray energies $E_\gamma \geq 40$ MeV was approximately 50% for all the targets at 195 MeV. This value was deduced by using the recent measurement of the π^0 cross section in proton induced reactions on several targets at an incident proton energy of 200 MeV by Bellini *et al.* [25]. The cross sections that we report here have been corrected for the π^0 contribution.

The angular distributions for the high energy photons from all the targets exhibited no quadrupole component. In fact the addition of the quadrupole term in Eqn. (2) would be rejected by the F-Test which checks the validity of an additional term in a least squares fit. On the basis of this test we can conclude that there is no strong

evidence for coherent photon production in proton induced reactions. The angular distribution in the nucleon-nucleon center-of-mass frame for the energy integrated cross section with photon energies, $E_\gamma \geq 40$ MeV for the targets are displayed in Fig. 3. The fits for the heavy targets are for isotropic plus dipole components in the emitting frame. Theoretical predictions for the shape of high energy gamma ray angular distributions are that it should be isotropic with dipole component [26–28]. Unlike the heavy targets, the C target exhibits a forward peaking in the nucleon-nucleon frame. In the nucleon–nucleon center-of-mass frame the ratio of cross section at the most forward angle to that at the most backward angle in the laboratory is 2.1 ± 0.1 for the C target and 1.1 ± 0.1 for the Pb target at 145 MeV. This strong forward peaking in the nucleon-nucleon frame could be due to an asymmetry in the reaction. In heavy-ion collisions the total interaction is an average over target neutrons target interacting with projectile protons and similarly target protons colliding with projectile neutrons. In proton–nucleus reactions, the only contribution to the interaction is from propton collisions with neutrons from the target, and the angular distribution should reflect this asymmetry. One other possible explanation might be the importance of multi-step processes in gamma ray production in which the incident proton suffers one or more collisions before creating the bremsstrahlung photon, such an idea might explain the difference in the angular distributions between the light and heavy targets. This point needs further investigation.

B. Comparison with Other Data

In order to obtain a more qualitative understanding of the systematics of the several experimental data sets, a reasonable method of comparing the energy spectra was required. The energy spectra for the Edgington and Rose data [13] as well as those of Kwato *et al.* [14] and Pinston *et al.* [15] are plotted in Fig. 4 versus a

reduced variable E_γ/E_p, which is the ratio of measured gamma ray energy divided by the incident proton energy. The agreement between the present data at 104 and 145 MeV as well as the data from Kwato *et al.* and Pinston *et al.* is clearly displayed. There is a discrepancy between the data of Kwato *et al.* at 72 MeV and the remaining measurements for the C target which may be due to incomplete rejection of the background from fast particles or a gain shift in their NaI(Tl) detector for this portion of the experiment. There is a constant difference of about a factor of 2-3 that is observed in comparison to the Edgington and Rose data for all the targets. Such a result was reported earlier by Kwato *et al.* . A more quantitative approach to explore the discrepancies between the Edgington and Rose cross sections and the other measurements is to compare the total cross section above a low energy threshold. Total cross sections were found by integrating the double differential cross section above 40 MeV and then multiplying the resultant by 4π, this same procedure that was used in the previous measurements [14, 15]. The results are displayed in Table II and Table III. As can be seen from Table III there is reasonable agreement between the measurements by Kwato *et al.* and Pinston *et al.* and the present work. However, the ratio between the cross sections obtained by Edgington and Rose at 140 MeV and the present data at 145 MeV is 2.9 ± 0.6 which is similar to the discrepency reported by Kwato *et al.* . The results from Table II and Table III are summarized in Fig. 5 which is a plot of the probability of gamma ray emission P_γ, for gamma ray energies $E_\gamma \geq 40$ MeV, versus the incident proton energy. The concept of P_γ was proposed by Nifenecker and Bondorf [26] as a way to look for systematic trends in gamma ray production in heavy-ion reactions and has been extended to proton nucleus collisions by Pinston *et al.* [15]. Under the assumption that the high energy gamma rays come from proton–neutron collisions, the production cross section can be written as:

$$\sigma_\gamma = \sigma_R P_n P_\gamma \tag{3}$$

where σ_R is the total reaction cross section [29], and P_γ is the probability to produce a single photon in an individual proton–neutron collision. P_n is the probability of the incident proton to undergo a collision with a neutron from the target and is given by:

$$P_n = \frac{N\sigma_{pn}}{N\sigma_{pn} + Z\sigma_{pp}} \tag{4}$$

Experimentally, Hess found that $\sigma_{pn} \approx 3\sigma_{pp}$ [30], and with this simplification Eqn. (3) can be rewritten as:

$$P_\gamma = \frac{\sigma_\gamma}{\sigma_R} \cdot \left(1 + \frac{Z}{3N}\right) \tag{5}$$

where N and Z are the number of neutrons and protons in the the target nucleus. Fig. 5 shows that there is reasonable agreement between the more recent works of Kwato *et al.* and Pinston *et al.* compared with the present data. It should be noted that the data at 195 and 200 MeV are not as precise as the lower energy data due to the large uncertainty in the π^0 subtraction. Even so, there is a linear increase of P_γ as the incident proton energy is increased.

IV. CONCLUSIONS

High energy gamma ray production was studied using proton beams at 104, 145 and 195 MeV on target of C, Zn and Pb. We find reasonable agreement with the measurements from Kwato *et al.* and Pinston *et al.* . Conversely all of these are in disagreement with the earlier work on bremsstrahlung gamma ray production from Edgington and Rose. We have used a simple asymptotic formulation of proton-neutron bremsstrahlung cross section from Nakayama and Bertsch, and we find that it is a reasonable parameterization of the heavier target data. However, the least-squares fit to the C target is not very good, and it may be that this simple model is not applicable to lighter systems where proper phase space treatment is required. We find that the source velocities are consistent with emission from a moving source at the

nucleon-nucleon center-of-mass velocity. We also find no evidence for any collective bremsstrahlung in the data, based on the observed angular distribution for these high energy photons.

V. ACKNOWLEDGEMENTS

The authors would like to thank the operations group at IUCF for their competent collaboration during the experiment. The authors would like to thank Professor George Bertsch and Professor Wolfgang Bauer for their valuable advice. This work was supported in part by grant PHY89-13815 from the National Science Foundation.

REFERENCES

* On leave from Dept. of Physics, Chalmers Univ. of Tech., S-412 96 Göteborg, Sweden.

† Present address: Lawrence Livermore National Laboratory, Livermore, CA 94550.

‡ Present address: Laboratoire de Physique Nucléaire, Univ. de Nantes, 2 rue de la Houssiniáre, 44072 Nantes Cèdex 03, France

§ Present address: Science Applications International Corporation, 2950 Patrick Henry Drive, Santa Clara, CA 95054

[1] K. B. Beard, W. Benenson, C. Bloch, E. Kashy, J. D. Stevenson, D. J. Morrissey, J. van der Plicht, B. Sherrill, and J. S. Winfield, *Phys. Rev.* **C32**, 1111 (1985).

[2] E. Grosse, P. Grimm, H. Heckwolf, W. F. J. Mueller, H. Noll, A. Oskarsson, H. Stelzer, and W. Rosch, *Europhysics Lett.* **2** 9 (1986).

[3] N. Alamanos, P. Braun-Munzinger, R.F. Freifelder, P. Paul, J. Stachel, T. C. Awes, R. L. Ferguson, F. E. Obenshain, F. Plasil and G.R. Young, Phys. Lett. **173B**, 392 (1986).

[4] M. Kwato Njock, M. Maurel, E. Monnand, H. Nifenecker, J. Pinston, F. Schussler, and D. Barneoud, *Phys. Lett.* **175B**, 125 (1986).

[5] J. D. Stevenson, K. B. Beard, W. Benenson, J. Clayton, E. Kashy, A. Lampis, D. J. Morrissey, M. Samuel, R. J. Smith, C. L. Tam, and J. S. Winfield, *Phys. Rev. Lett.* **57**, 555 (1986).

[6] R. Hingmann, W. Kuhn, V. Metag, R. Muhlhans, R. Novotny, A. Ruckelshausen, W. Cassing, B. Haas, H. Emling, R. Kulessa, H. J. Wollersheim, J. P. Vivien, A. Boullay, H. Delagrange, H. Doubre, C. Gregoire, e, Y. Schutz, *Phys. Rev. Lett.* **58**, 759 (1987).

[7] B. A. Remington, M. Blann, G. F. Bertsch, *Phys. Rev.* **C35**, 1720 (1987).

[8] W. Bauer, G. F. Bertsch, W. Cassing, and U. Mosel, *Phys. Rev.* **C34**, 2127 (1986).

[9] K. Nakayama and G. F. Bertsch, *Phys. Rev.* **C34**, 2190 (1986).

[10] F. P. Brady and J. C. Young, *Phys. Rev* **C2**, 1579 (1970).

[11] J. A. Edgington, V. J. Howard, I. M. Blair, B. E. Bonner, F. P. Brady and M. W. McNaughton, *Nucl. Phys.* **A218**, 151 (1974).

[12] C. Dupont, C. Deom, P. Leleux, P. Lipnik, P. Macq, A. Ninane, J. Pestieau, S. W. Kitwanga and P. Wauters, *Nucl. Phys.* **A481**, 424 (1988).

[13] J. A. Edgington and B. Rose, *Nucl. Phys.* **89**, 523 (1966).

[14] M. Kwato Njock, M. Maurel, H. Nifenecker, J. Pinston, F. Schussler, D. Barneoud, S. Drissi, J. Kern, and J. P. Vorlet *Phys. Lett.* **207B**, 269 (1988).

[15] J. A. Pinston, D. Barneoud, V. Bellini, S. Drissi, J. Guillot, J. Julien, M. Kwato Njock, H. Nifenecker, M. Maurel, F. Schussler, and J. P. Vorlet *Phys. Lett.* **218B**, 128 (1989).

[16] R. Bertholet, M. Kwato Njock, M. Maurel, E. Monnand, H. Nifenecker, P. Perrin, J. A. Pinston, F. Schussler, D. Barneoud, C. Guet and Y. Schutz, *Nucl. Phys.***A474**, 541 (1987).

[17] P. F. M. Koehler, K. W. Rothe and E. H. Thorndike, *Phys. Rev. Lett.* **18**, 933 (1967).

[18] Supplied by Englehard Corp., Solon, OH

[19] J. Clayton, J. D. Stevenson,W. Benenson, D. Krofcheck, D. J. Morrissey, T. K. Murakami and J. S. Winfield, *Phys. Rev.* **C42**, 1009 (1990).

[20] Supplied by McGhan-Nusil Corp., CA

[21] *The EGS4 Code System*, W. R. Nelson, H. Hirayama and D. W. O. Rogers, *SLAC-265 UC-32*, Stanford Linear Accelerator Center, Stanford University, Stanford CA, 94305 (1985).

[22] J. Clayton, W. Benenson, N. Levinsky, M. F. Mohar, J. D. Stevenson, E. Hallin, J. Bergstrom, H. Caplan, R. Pywell, D. Skopik and J. Vogt, *Nucl. Instr. and Meth.* **A305**, 116 (1991).

[23] A. L. Fetter, J. D. Walecka, *Quantum Theory of Many–Particle Systems*, McGraw–Hill Book Co., New York, 145 (1971).

[24] code *MINUIT*, D506, CERN Program Library.

[25] V. Bellini, M. Bolore, J. Julien, J. M. Hisleur, A. Fallica, A. S. Figuera, R. Fonte, A. Insolia, C. Milone, G. F. Palama, G. V. Russo, M. L. Sperduto, and L. Bimbot, *Zeitschrift für Phys.* **A333**, 393 (1989).

[26] H. Nifenecker, and J. P. Bondorf, *Nucl. Phys.* **A442**, 478 (1985)

[27] W. Bauer, W. Cassing, U. Mosel and M. Tohyama *Nucl. Phys.* **A456**, 159 (1986).

[28] V. Herrmann, J. Speth and K. Nakayama, *Phys. Rev* **C43**, 394 (1991).

[29] W. Bauhoff *Atomic and Nucl. Data Tables* **35**, 429 (1986).

[30] W. N. Hess, *Rev. Mod. Phys.* **30**, 368 (1958).

FIGURES

FIG. 1. Gamma ray energy spectra in the laboratory frame for 104 (upper frame) and 145 MeV (lower frame) protons incident on a lead target at three of the measured angles.

FIG. 2. A comparison of the measured energy spectra for the C (lower frame) and Pb (upper frame) targets and the results of a least-squares fit to the data by the function given in Equation 2 at 45°, 90° and 135° in the laboratory frame.

FIG. 3. Angular distributions for all the targets measured at 104 and 145 MeV in the nucleon-nucleon center-of-mass frame. The low energy cutoff is 40 MeV in this frame.

FIG. 4. A comparison of the energy spectra for C, Zn, Pb targets at 104 and 145 MeV to the data from Kwato *et al.* [14] at 72 MeV, Edgington and Rose [13]at 140 MeV and Pinston *et al.* [15] at 168 MeV versus a reduced variable, E_γ/E_p which is the measured gamma ray energy divided by the incident proton energy.

FIG. 5. A plot of the probability of gamma ray emission P_γ in a proton-neutron collision. The low energy cut is for gamma ray with energies $\geq$ 40 MeV. The data points are plotted from the present work and Refs. [14, 15] for various targets.

TABLES

TABLE I. Source velocities extracted from the rapidity distribution plots. The cuts in energy are listed.

E_p = 104 MeV β_{nn} = 0.23				
Target	E_γ=25 MeV	E_γ=50 MeV	E_γ=75 MeV	
	β	β	β	
Carbon	0.16 ± 0.03	0.18 ± 0.03	0.15 ± 0.05	
Zinc	0.17 ± 0.03	0.20 ± 0.03	0.18 ± 0.05	
Lead	0.14 ± 0.03	0.19 ± 0.03	0.17 ± 0.05	
Mean Value	0.16	0.19	0.17	
E_p = 145 MeV β_{nn} = 0.27				
Target	E_γ=25 MeV	E_γ=50 MeV	E_γ=75 MeV	E_γ=100 MeV
Carbon	0.22 ± 0.03	0.21 ± 0.03	0.21 ± 0.04	0.19 ± 0.05
Zinc	0.14 ± 0.03	0.23 ± 0.03	0.22 ± 0.04	0.22 ± 0.05
Lead	0.21 ± 0.03	0.25 ± 0.03	0.25 ± 0.04	0.23 ± 0.05
Mean Value	0.19	0.23	0.23	0.21

TABLE II. Comparison of the total cross section for gamma rays with $E_\gamma \geq 40$ MeV from 140 MeV protons on various targets to the present data at 145 MeV. The values for the cross section at 140 MeV are from the work of Edgington and Rose [13].

Present Data			Edgington and Rose		
E_p	Target	σ_{tot}	E_p	σ_{tot}	Ratio
MeV		μb	MeV	μb	
145	C	57 ± 6	140	23 ± 3	2.48
145	Zn	282 ± 29	140	80 ±10[a]	3.53
145	Pb	612 ± 61	140	224 ± 27	2.73
					Mean Value 2.9 ± 0.6

[a] Results with a Cu target

TABLE III. A comparison of the total cross section of gamma rays above 40 MeV from proton induced reactions at incident energies of 72, 104, 168, 195, and 200 MeV [14, 15].

E_p (MeV)	Target	σ_{tot} (μb)	Reference
72	C	23 ± 2	Kwato *et al.*
72	Cu	59 ± 6	
72	Au	94 ± 9	
104	C	35 ± 4	Present data
104	Zn	144 ± 15	
104	Pb	327 ± 33	
168	C	90 ± 9	Pinston *et al.*
168	Al	221 ± 22	
168	Cu	361 ± 36	
168	Ag	606 ± 61	
168	Tb	806 ± 81	
168	Au	911 ± 91	
195	C	179 ± 30	Present data
195	Zn	665 ± 120	
195	Pb	1695 ± 300	
200	C	155 ± 32	Pinston *et al.*
200	Ag	1049 ± 208	
200	Au	910 ± 269	

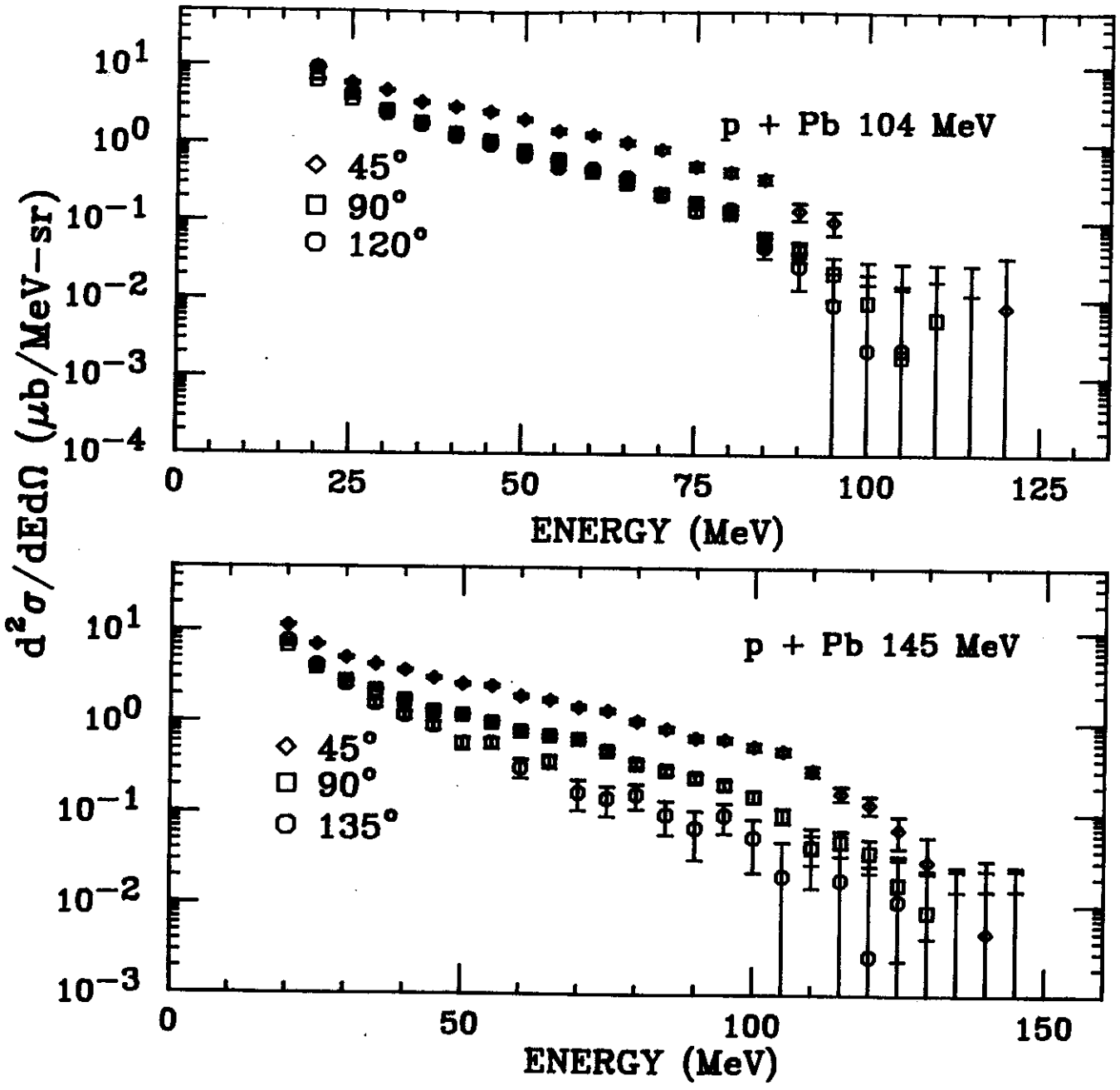
p + Pb 104 MeV
45°
90°
120°
p + Pb 145 MeV
45°
90°
135°
d²σ/dEdΩ (μb/MeV-sr)
ENERGY (MeV)
ENERGY (MeV)

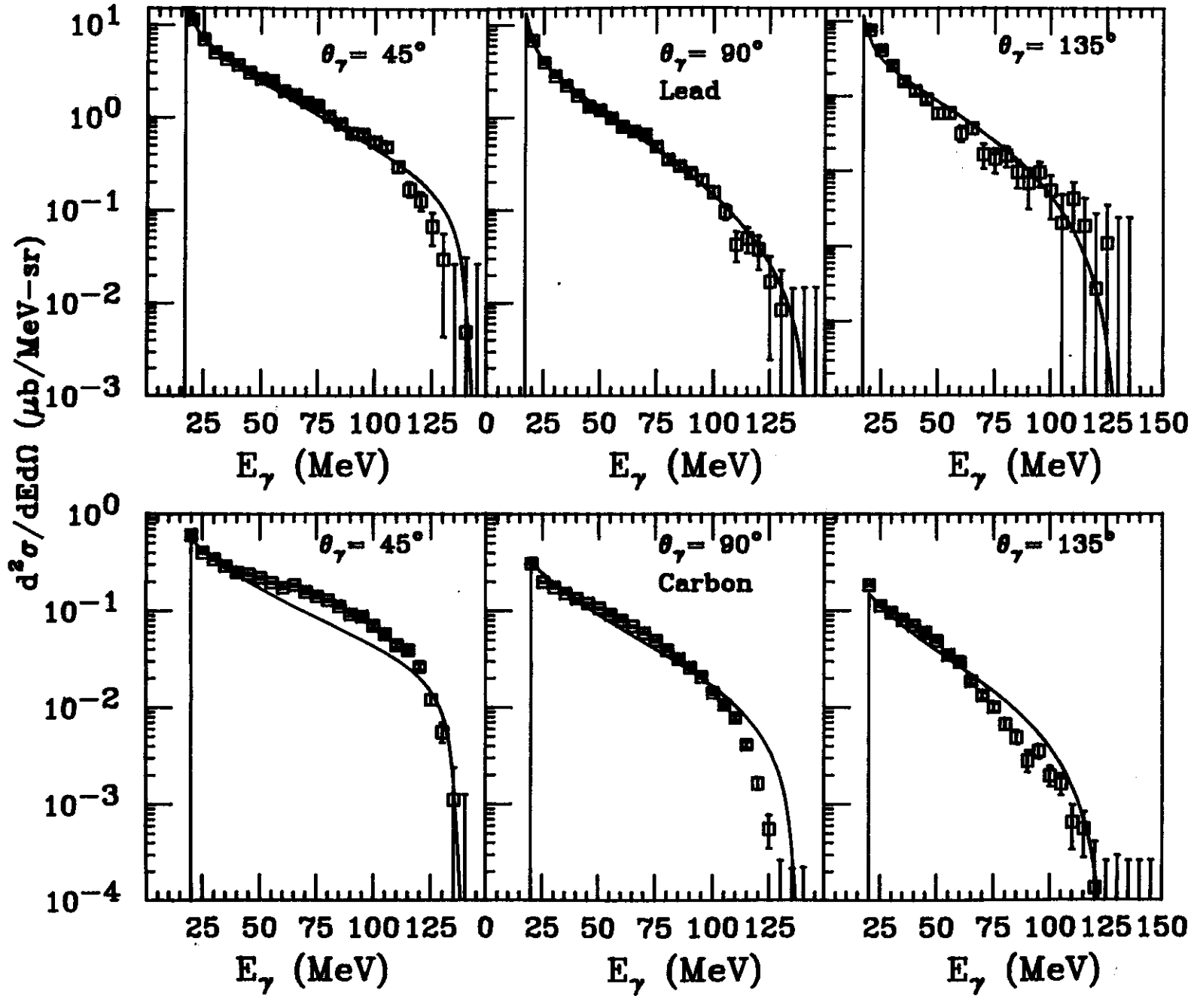
θ_γ= 45°
θ_γ= 90°
Lead
θ_γ= 135°
θ_γ= 45°
θ_γ= 90°
Carbon
θ_γ= 135°
$d^2\sigma/dEd\Omega$ (μb/MeV-sr)
E_γ (MeV)
E_γ (MeV)
E_γ (MeV)
E_γ (MeV)
E_γ (MeV)
E_γ (MeV)

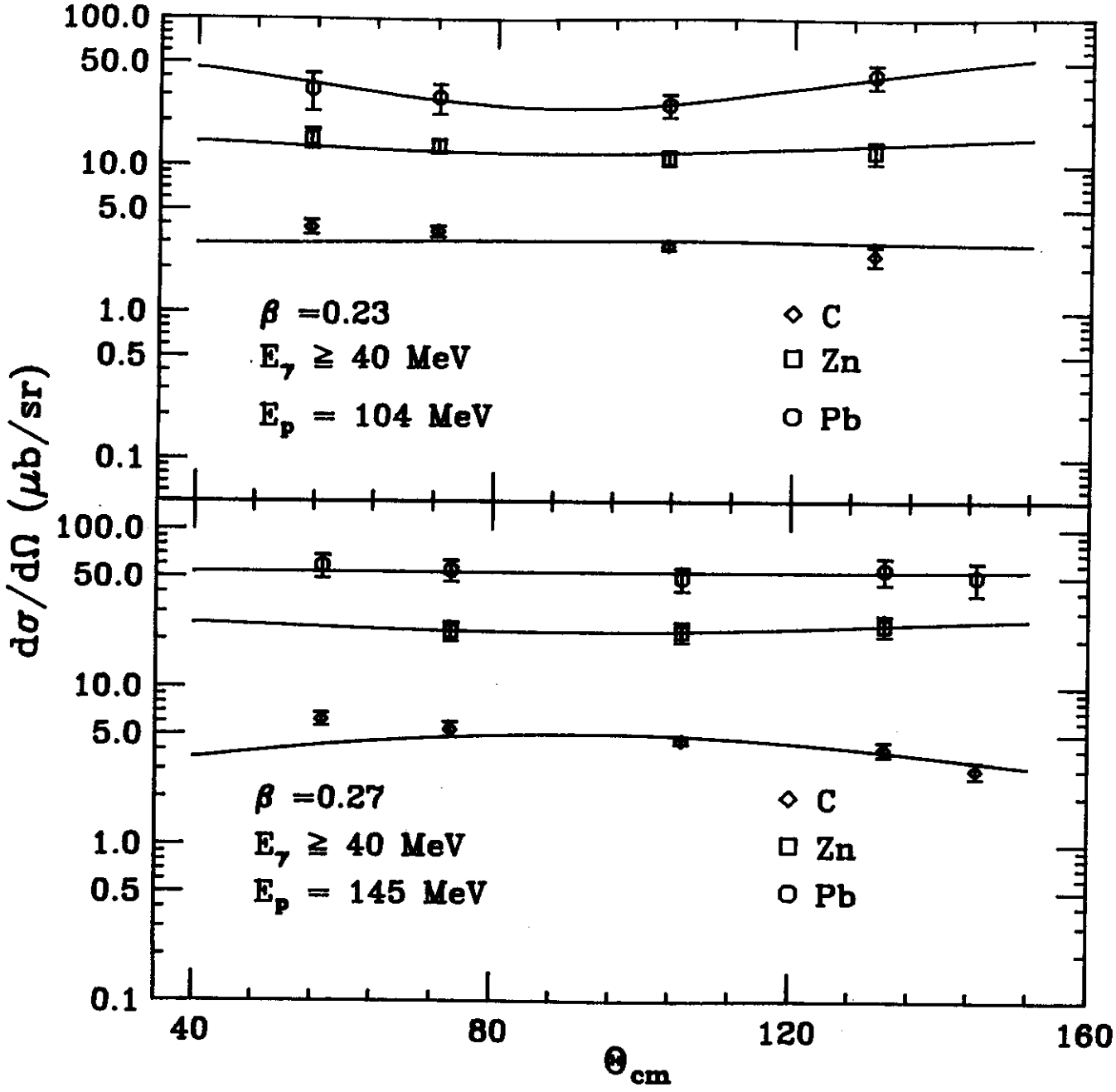
100.0
50.0
10.0
5.0
1.0
0.5
0.1
β =0.23
E_γ ≥ 40 MeV
E_p = 104 MeV
◇ C
□ Zn
○ Pb
100.0
50.0
10.0
5.0
1.0
0.5
0.1
β =0.27
E_γ ≥ 40 MeV
E_p = 145 MeV
◇ C
□ Zn
○ Pb
dσ/dΩ (μb/sr)
40
80
120
160
Θ_cm

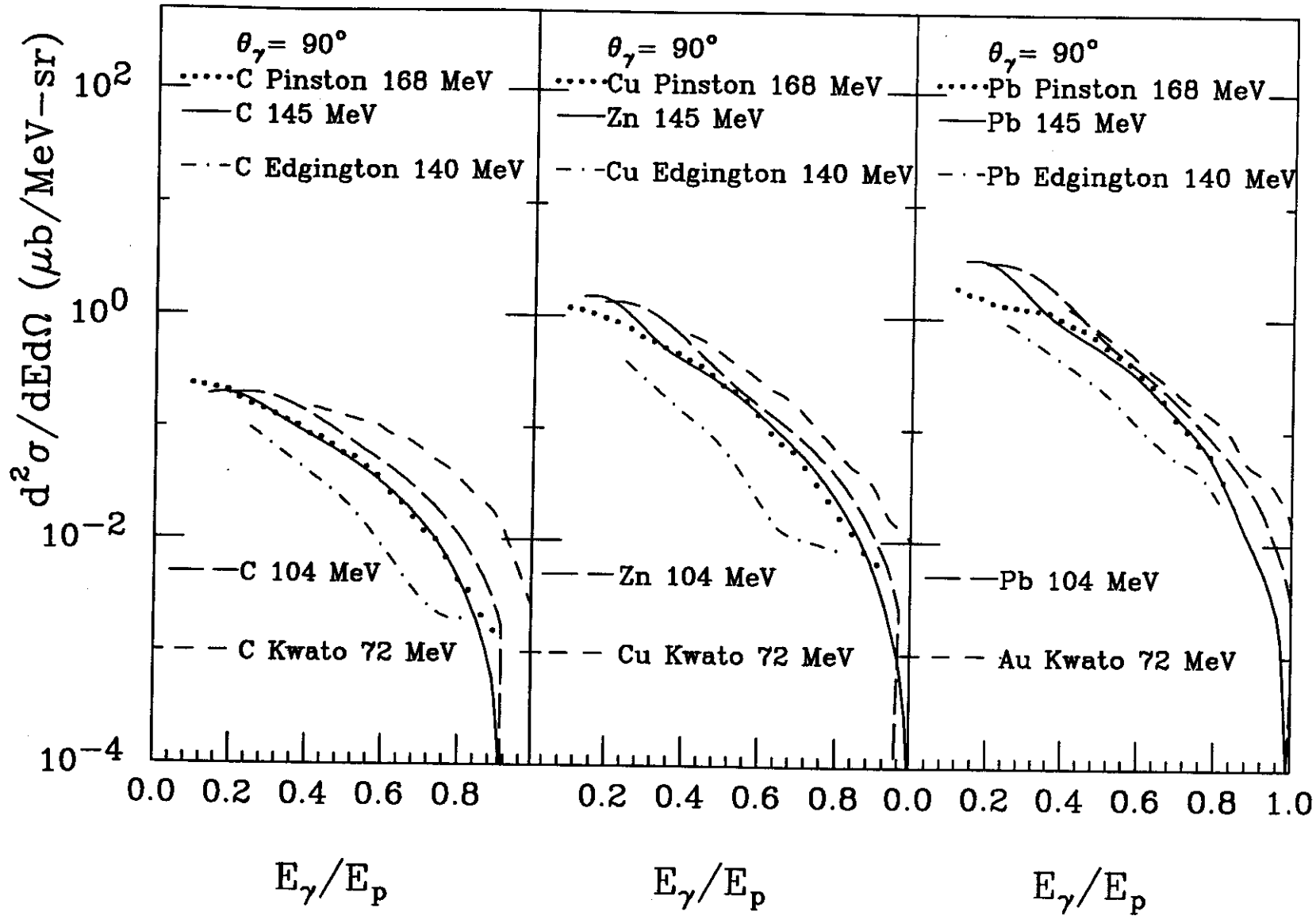
θ_γ= 90°
C Pinston 168 MeV
C 145 MeV
C Edgington 140 MeV
C 104 MeV
C Kwato 72 MeV
Cu Pinston 168 MeV
Zn 145 MeV
Cu Edgington 140 MeV
Zn 104 MeV
Cu Kwato 72 MeV
Pb Pinston 168 MeV
Pb 145 MeV
Pb Edgington 140 MeV
Pb 104 MeV
Au Kwato 72 MeV
$d^2\sigma/dEd\Omega$ (μb/MeV−sr)
10^2
10^0
10^{-2}
10^{-4}
0.0 0.2 0.4 0.6 0.8
0.2 0.4 0.6 0.8 0.0 0.2 0.4 0.6 0.8 1.0
E_γ/E_p
E_γ/E_p
E_γ/E_p

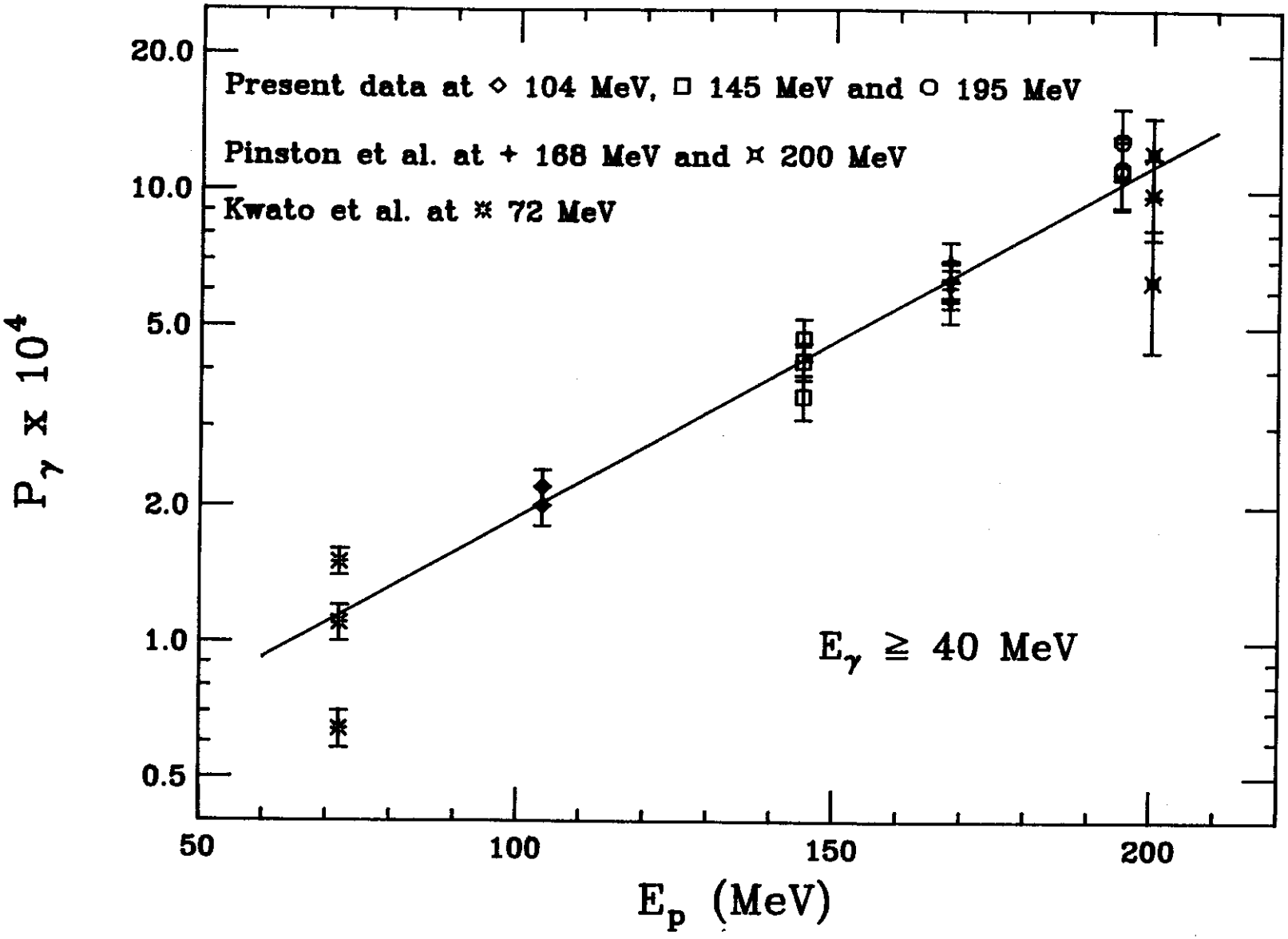
Present data at ◇ 104 MeV, □ 145 MeV and ○ 195 MeV
Pinston et al. at + 168 MeV and ⋈ 200 MeV
Kwato et al. at ⋇ 72 MeV
$E_\gamma \geqq 40$ MeV
$P_\gamma \times 10^4$
E_p (MeV)
20.0
10.0
5.0
2.0
1.0
0.5
50
100
150
200